e-ISSN: 2550-164X

Available online at
https://jmeche.uitm.edu.my/

Journal of Mechanical Engineering 22(1) 2025, 90 – 103

Journal of Mechanical Engineering

Effect of Implant Positioning in Cemented Hip Arthroplasty

Zaitul Asyikin Aznan[1], Nur Maisarah Khairul Azahan[1], Shahrul Hisyam Marwan[2], Mohamad Taufiqurrakhman[3,4], Hemant Pandit[3], Thawhid Khan[4], Abdul Halim Abdullah[1*]

[1]*School of Mechanical Engineering, College of Engineering, Universiti Teknologi MARA (UiTM), 40450 Shah Alam, Selangor, Malaysia*
[2]*School of Mechanical Engineering, College of Engineering,Universiti Teknologi MARA (UiTM) Terengganu Branch, Bukit Besi Campus, 23200 Dungun, Terengganu, Malaysia*
[3]*Leeds Institute of Rheumatic and Musculoskeletal Medicine (LIRMM), School of Medicine, University of Leeds, Leeds, LS9 7TF, UK*
[4]*Institute of Functional Surfaces (iFS), School of Mechanical Engineering, University of Leeds, Leeds, LS2 9JT, UK*

ARTICLE INFO

Article history:
Received 15 August 2024
Revised 9 September 2024
Accepted 14 October 2024
Online first
Published 15 January 2025

Keywords:
Total hip arthroplasty (THA)
Implant positioning
Cement mantle
Finite element analysis
Varus plane

DOI:
10.24191/jmeche.v22i1.2802

ABSTRACT

The positioning of a cemented total hip arthroplasty (THA) is a crucial factor during the surgical implantation procedure. However, the impact of misalignment on stress distribution at the cement mantle and bone remains poorly understood, posing a potential risk for periprosthetic bone fracture. This study explores the effects of hip stem positioning in cemented THA by using finite element analysis (FEA). The aim is to investigate the impact of implant position on stress and deformation distributions at the contacting components, i.e. femoral bone, cement, and hip stem, under walking and stair-climbing activity's forces. The rotating angles of -0.75°, -0.5°, -0.25°, 0.25°, 0.5°, and 0.75° are used at the varus plane with the distal end of the stem as the centre of rotation. The unrotated condition (at an angle of 0°) is simulated as the baseline condition of normal hip stem position. Results indicate that the baseline angle of 0° position does not necessarily represent the lowest stress and deformation in the femoral bone. Furthermore, misalignment angle variations at varus planes minimally affect total deformation but significantly impact stress distribution at the cement mantle. These findings underscore the importance of considering alignment angles beyond the baseline and their effects on stress and deformation in cemented THA.

INTRODUCTION

The field of medical practice has seen tremendous improvement over the years. These improvements have been made possible with the inclusion and application of mechanical input and technology which could alleviate the patient's suffering. The mechanical aspect includes the design of several contraptions,

[1*] Corresponding author. *E-mail address*: halim471@uitm.edu.my
https://doi.org/10.24191/jmeche.v22i1.2802

implants, or devices that could be inserted into the patient's body to ease the pain. This paper discusses the subject of total hip arthroplasty (THA), a study of medical remedies to reduce pain in the hip area by using implants. The most common techniques of fixation in THA are cement and cementless (Apostu et al., 2018). However, this paper will focus on cemented hip implants. In cemented hip arthroplasty operation, it involves the effects of implant positioning which would enable the patient to walk unassisted and also lessen their suffering (Gómez Alcaraz et al., 2021).

One of the biggest and most crucial joints in the human body is the hip joint. The articulation of the femur (thigh bone) with the acetabulum, a concave socket in the pelvis, results in a ball and socket joint (Glenister et al., 2024). A complex network of muscles, tendons, and ligaments stabilize and enable mobility while supporting the hip joint (Tamaki et al., 2022). Currently, the number of patients undergoing THA continues to rise especially among the senior population (Gómez Alcaraz et al., 2021). THA is a medical surgery that requires some delicate operation and also involves the insertion and placing of an implant in the hip area. In other words, THA is a replacement of a joint surgery that requires an acetabular and a femoral component that must be attached to the pelvic and femoral bones to achieve the ideal positioning for the prosthesis's optimal performance (Torini et al., 2023).

In detail, THA involves the removal of layers of the hip socket through an incision made above the head and proximal neck of the femur. Then, a plastic socket is fitted into the expanded pelvis cup, and a metal ball and stem are implanted into the femur (Ahmad et al., 2020). THA entails loosening the iliofemoral ligament to obtain access to the femoral head and neck (Ng et al., 2019). THA is one of the methods that can be used to treat diseases like osteoarthritis, rheumatoid arthritis, or injuries that can cause the articular cartilage to degenerate, resulting in discomfort, stiffness, and a loss of function (Ng et al., 2019). The most prevalent type of joint condition is osteoarthritis (OA), which is also known as "wear-and-tear" arthritis, age-related arthritis, or degenerative joint disease (Abdelaal et al., 2021). One way to understand it is that OA is a form of arthritis that presents itself most frequently in the hips, knees, feet, and wrists causing discomfort in the joints and restricting movement in those areas (Yue & Berman, 2022). About 150 million people around the world which consists mainly adults and senior citizens are affected by this condition, which causes pain and disability (Torini et al., 2023). Patients experiencing hip osteoarthritis commonly demonstrate an irregular spine-hip relation (SHR), indicative of the presence of clinically detrimental spine-hip and/or hip-spine syndromes (Rivière et al., 2018).

The degenerative changes in joint tissues that lead to structural changes in the articular cartilage and subchondral bone are what distinguish OA from other joint diseases (Whittaker et al., 2021). There are two classifications of OA which are primary and secondary. Primary OA typically affects many joints in the general senior population and is of idiopathic origin. Secondary OA is typically monoarticular and caused by a joint articular disease such as trauma (Abdelaal et al., 2021). However, the incidence of hip OA continues to rise due to the aging of society and also the increase in obesity (Miller et al., 2018). Several factors must be considered in THA including implant design, materials, and fixation (Ahmad et al., 2020). There are two main techniques of fixation in THA which are cement and cementless (Apostu et al., 2018). Polymethylmethacrylate (PMMA) is the bone cement that is most frequently utilized during THA (Zheng et al., 2021). However, the cementless relies on the biological fixation of bone to a prosthetic implant's surface (Maggs & Wilson, 2017). The age of the patient and the quality of the bone will also determine the method of fixation that will be used (Katz et al., 2018). Cementless fixation is preferred for patients who are younger and more active (Ahmad et al., 2020). Cemented implants tend to be the most preferable method for older people (Katz et al., 2018).

PMMA is used as grout in cemented THA, which creates an interlocking fit between the cancellous bone and the prosthesis (Maggs & Wilson, 2017). PMMA is also a bioinert substance that does not chemically or biologically bind with host bone at the interface (Zheng et al., 2021). PMMA offers numerous benefits including biocompatibility, ease of handling, processability, and low cost (Ramanathan et al., 2024). There are two main categories of cemented stems which are taper-slip and composite beam (Maggs

https://doi.org/10.24191/jmeche.v22i1.2802

& Wilson, 2017). In THA, "implant stability" is described as the orientation and position of the implant during primary fixation between the prosthesis stem and the longitudinal axis of the femur (Yusof et al., 2021). Implantation accuracy is measured as the deviation between the target stem anteversion angle and postoperative computed tomography measurements of stem anteversion (Mitsutake et al., 2020). The distal section of the implant being either medial or the side from its normal state led to the determination of the varus position of the implant in THA (Yusof et al., 2021). For the THA to be biomechanically stable, the acetabular component must be positioned correctly (Torini et al., 2023). This is because the stress distribution is affected by the modification of implant position in the varus and sagittal planes, which also contributes to bone adaptation and stress shielding effects (Yusof et al., 2021).

The main purposes of this project are to develop the finite element model of cemented hip arthroplasty at varus implant positioning and to analyze the effect of hip implant positioning on the distribution of stresses and total deformation. The scope of the project will be restricted to a computational analysis utilizing FEA and will not encompass any actual verification or medical assessments. Therefore, this study will not include any specific patient correlated with this problem. The precision of the FEA outcomes is based on the input parameters and assumptions applied in the simulation, which could potentially impose certain constraints.

METHODOLOGY

A combination of computer-aided design (CAD) and finite element analysis (FEA) techniques through commercial finite element software were employed to explore the effects of hip stem positioning in cemented THA. Fig 1 depicts a schematic of the detailed research methodology conducted in this study.

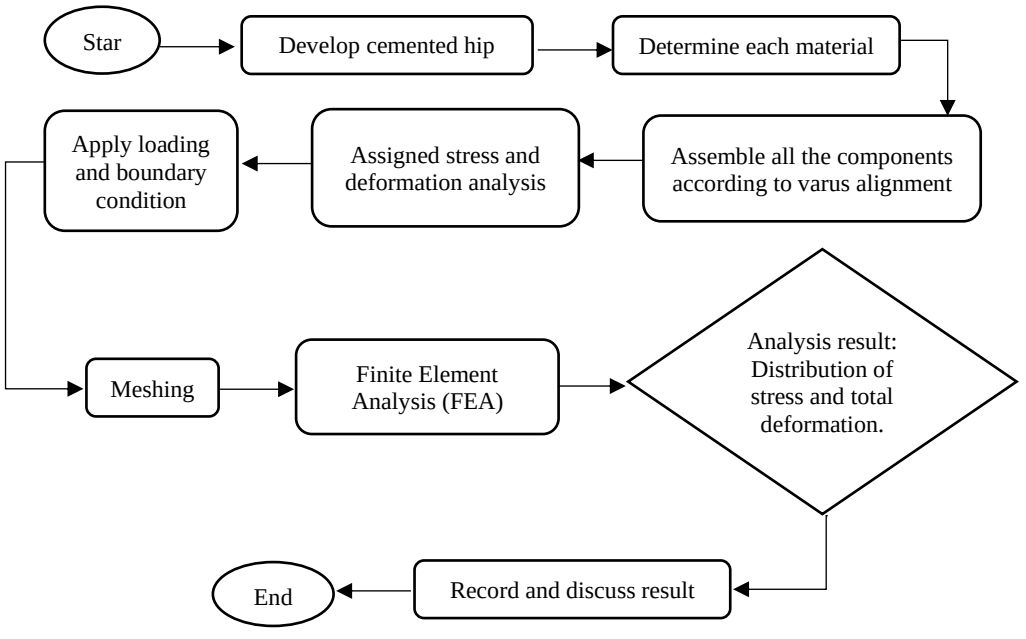

Fig. 1. Schematic of CAD modeling and FEA developments.

https://doi.org/10.24191/jmeche.v22i1.2802

Finite element model

CAD model

This study used a cemented THA model that consisted of three main components, i.e. hip prosthesis stem, cement mantle, and femoral bone as shown in Fig 2. Computed tomography (CT) was employed to obtain three-dimensional (3D) imaging and a model to be simulated in this study (Kim & Jung, 2013). Commercial medical software processes this information to integrate prosthetics accurately. This study used CT imaging from cadaveric samples to generate a 3D model of the femoral bone, provided by the University Malaya Medical Centre (UMMC) with a 0.75 slice thickness. The bone cement model has a distal thickness of 20 mm and a surrounding thickness of 2 mm (Ahmad et al., 2020).

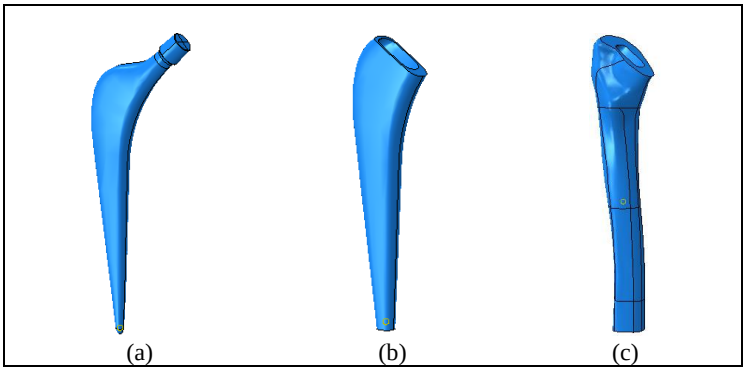

Fig. 2. Components in 3D model visualization; (a) cemented hip stem, (b) cement mantle, and (c) femoral bone.

Material properties

In order to obtain an accurate model, material properties were assigned for each component, as shown in Table 1. In this study, the femoral bone was made of cortical and cancellous bones, whereas polymethyl methacrylate (PMMA) material was used for the cement mantle (Ahmad et al., 2020). The cemented hip stem was assumed to be made of biocompatible stainless steel, which was known for its remarkable resistance to corrosion and superior strength (Olugbade, 2022).

Table 1. Material properties (Ahmad et al., 2020; JMS, 2014)

Components	Materials	Young modulus, E (GPa)	Poisson's ratio	Yield strength (MPa)
Femoral bone	Corticol bones	17	0.3	115
	Cancellous bones	0.05	0.2	4.2
Cement mantle	PMMA	2	0.3	29
Hip stem	Stainless steel	200	0.28	205

Varus misalignments

The assembly process involved integrating cemented hip model components to possess varied scenarios of both normal and misaligned arthroplasty conditions. Detailed connections between these components simulate their interactions, facilitating accurate load transfer within the joint. The misalignment conditions included only the hip stem intentionally inclined with such angles of rotation at varus planes (Bini et al., 2021; Schwab, 2017). The distal end of the hip stem was used as the center of rotation, so that only the proximal/stem neck leaned to one side of the bone, creating an uneven cement mantle in between. Fig 3 illustrates when the hip stem and cement mantle at normal position (0°) and six different angles are applied to rotate the hip stem at varus plane (anterior view) i.e. -0.75°, -0.5°, -0.25°, 0.25°, 0.5°, and 0.75°.

https://doi.org/10.24191/jmeche.v22i1.2802

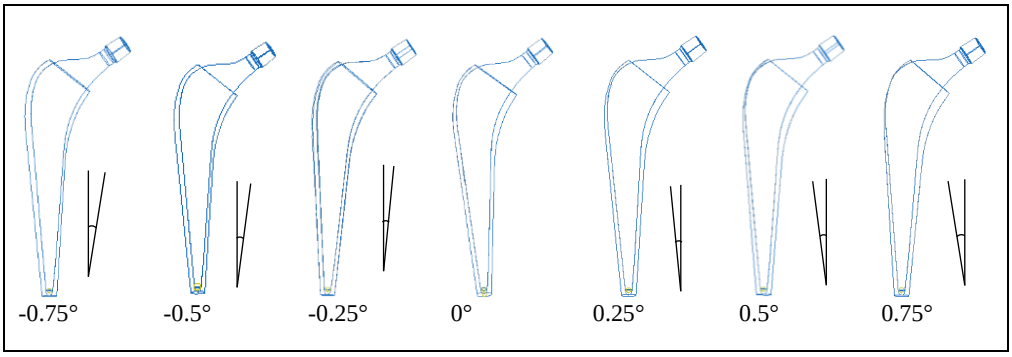

Fig. 3. Implant positioning in different angles at the varus plane (anterior view).

FEA parameter input

Step and model setup (interaction)

The 'Step' phase utilizes Abaqus software to evaluate implant positioning effects in the cemented hip arthroplasty. Output requested for *S* (stress components and invariants), MISES (Mises equivalent stress), and *U* (translations and rotations).

The interactions stage defined the model setup to iterate later the stress distribution and load transfer within the hip model. Surface contact constraints were integral, ensuring accurate biomechanical simulations in cemented hip arthroplasty within the FEA. “Tie” function was used in Abaqus software in order to fixate the parts of the bone and the cement, as well as the cement and the hip stem component.

Loading and boundary conditions

Forces and boundary conditions were applied by adapting the stair-climbing activity profile onto the hip model, as in the previous study (Ahmad et al., 2020). Two forces have been applied to the femur model which represents the hip loading (*P1*) and muscle reaction (*P2*), with a fixed load located at the bottom end as illustrated in Fig 4(a). This study explores the physiological loads associated with stair climbing to analyze the effect of hip implant positioning as shown in Table 2.

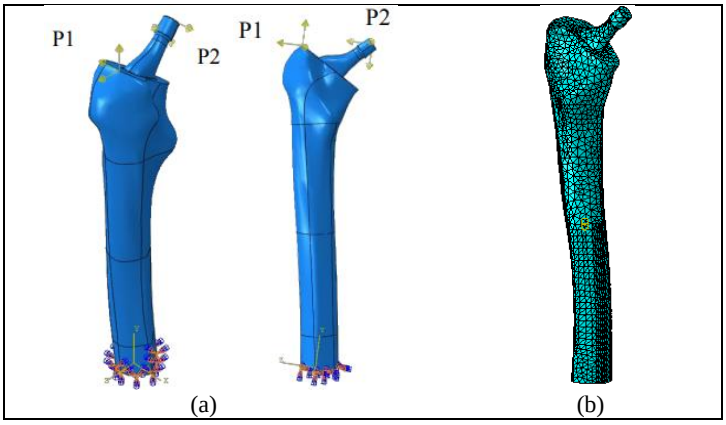

Fig. 4. (a) Location of each loading and boundary condition at different views and (b) meshing of cemented hip arthroplasty model.

https://doi.org/10.24191/jmeche.v22i1.2802

Table 2. Magnitude and direction of force applied (Ahmad et al., 2020).

Point	Forces	x	y	z
P1	Hip joint contact	-486.8	-1898.3	-476.4
P2	Abductor	231.4	682.1	563.1

Meshing

By incorporating global and local seeds, as well as utilizing tetrahedral elements, the meshing phase aimed to create an optimized mesh that sufficiently captures the structural intricacies and loading conditions specific to the cemented hip arthroplasty model. The mesh density was selected based on the previous study (Ahmad et al., 2020). The global seeds sized at 4 mm established baseline mesh density, capturing overall structural complexities. The local seed was set at 5 mm, further refining specific critical zones, like implant-bone interfaces or stress-prone areas. Abaqus primarily employs tetrahedral elements known for modelling intricate anatomical structures. Then, the meshing configuration will result in a pattern resembling that depicted in Fig 4(b).

FEA output visualization

This final phase encompassed executing Abaqus software to assess implant positioning effects in cemented hip arthroplasty. In the post-simulation, data on stress (von Mises) and deformation undergoes visualization using Abaqus tools to create graphical representations and contour plots. This analysis provided insights into how varus implant positions influence mechanical behavior under various loading scenarios.

RESULTS AND DISCUSSION

The study meticulously records the von Mises stress and magnitude deformation analyses for each individual material which are bone, cement, and the implant. The graphical representation vividly illustrates the comprehensive assessment of stress and deformation magnitudes within the examined materials. It shows a colour grading from dark blue representing the lowest values, to a spectrum of grey and red indicating the highest values.

Effects of hip stem misalignment at varus plane

Six angles (-0.75°, -0.5°, -0.25°, 0.25°, 0.5°, and 0.75) have been analysed in the context of varus alignment. Stress distribution analysis of all components colour-coded graphics in Fig 5 shows barely any variation in the distribution of stress at different angles. However, at the extremes of varus alignment (-0.75° and 0.75°), there appears to be a more pronounced concentration of stress along the medial and lateral aspects of the bone and implant which possibly indicates an uneven distribution of load due to the misalignment. High von Mises stress in the implant indicates that it is experiencing a significant load, which could exacerbate stress shielding in the surrounding bone. Whereas Fig 6 displays that the amount of deformation is relatively consistent across the range of angles, there might be a slightly greater deformation at the extreme varus angles particularly at -0.75°. At neutral alignment which is at 0°, the deformation is more evenly distributed throughout the length of all the components, which may indicate a more optimal load transmission through all the components which are implant, cement mantle, and femoral bone. In the context of THA, deformation results provide insight into how the bone and implant are displacing under load. High deformation in the implant shows that it is taking too much load, resulting in stress shielding.

https://doi.org/10.24191/jmeche.v22i1.2802

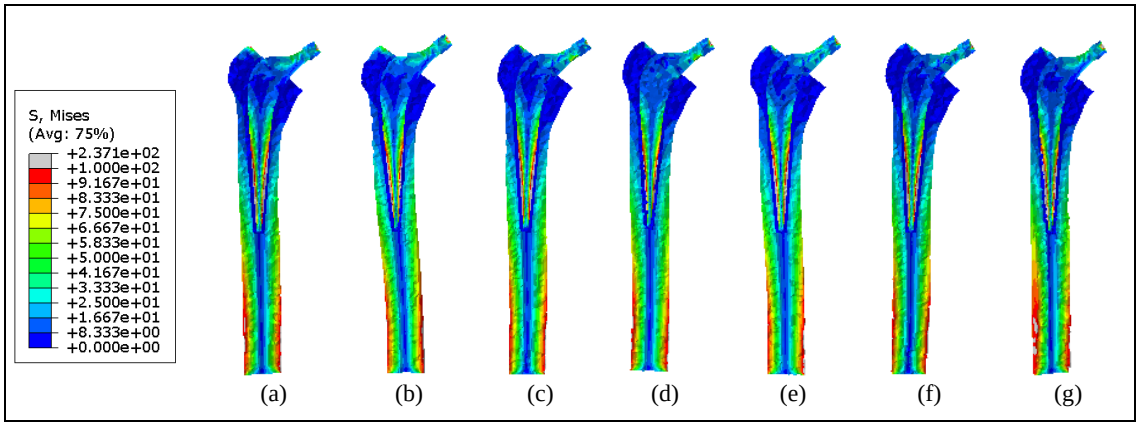

Fig. 5. Stress distribution analysis for all components at different varus angles (a) -0.75°, (b) -0.5°, (c) -0.25°, (d) 0°, (e) 0.25°, (f) 0.5°, and (g) 0.75°.

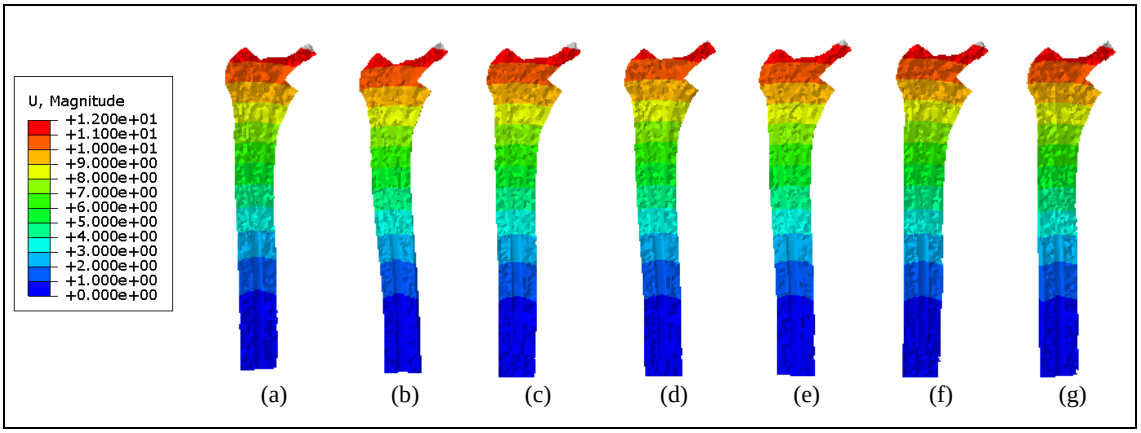

Fig. 6. Total deformation analysis for all components at different varus angles (a) -0.75°, (b) -0.5°, (c) -0.25°, (d) 0°, (e) 0.25°, (f) 0.5°, and (g) 0.75°.

Then, there is a slight variation in colours across different varus angles suggesting a change in the stress distribution pattern for the femoral bone as displayed in Fig 7. However, the overall stress distribution remains fairly consistent. Fig 7 displays that higher stress concentration at the lower part of the bone, which is somewhat distant from the typical location of the implant in a hip arthroplasty. Therefore, given that the higher stress is not in the immediate vicinity of the implant, the distribution could be influenced by the way the bone naturally distributes load, especially considering the altered biomechanics due to the varus alignment. The higher stress in the specific region encourages the thickening of bone (Yusof et al., 2021). Fig 8 reveals a consistently uniform deformation pattern across various angles for magnitude deformation analysis. This suggests that the varus positioning of the implant within the tested range has minimal influence on bone deformation during simulated physiological loads. This could imply that the bone's structural integrity is maintained across these alignment changes. Moreover, Fig 9 demonstrates that as the angle of varus increases from -0.75° to 0.75°, there is a slight decrease in von Mises stress. This might suggest that as the implant angle approaches the neutral which is at 0°, the stress on the femur decreases. However, the change in stress is very minimal, indicating that within the range of angles assessed, the stress distribution does not vary significantly. Fig 9 also shows that as the varus angle increases from -0.75° to

https://doi.org/10.24191/jmeche.v22i1.2802

0.75°, the magnitude of deformation reduces from 10.92 μm to 10.85 μm, implying that the femoral bone experiences less deformation as the implant angle moves towards the positive side. The trend is relatively linear, suggesting a predictable and proportional relationship between the varus angle and the deformation magnitude within the tested range. This information could be indicative of how the bone would behave under a load in real-world scenarios, where a slight variance in the angle of implantation could potentially affect the deformation experienced by the bone.

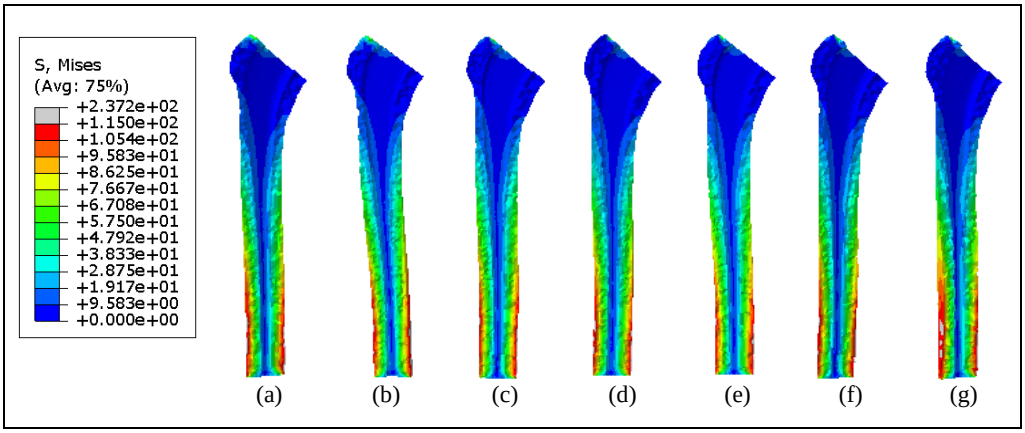

Fig. 7. Stress distribution analysis for femoral bone at different varus angles (a) -0.75°, (b) -0.5°, (c) -0.25°, (d) 0°, (e) 0.25°, (f) 0.5°, and (g) 0.75.

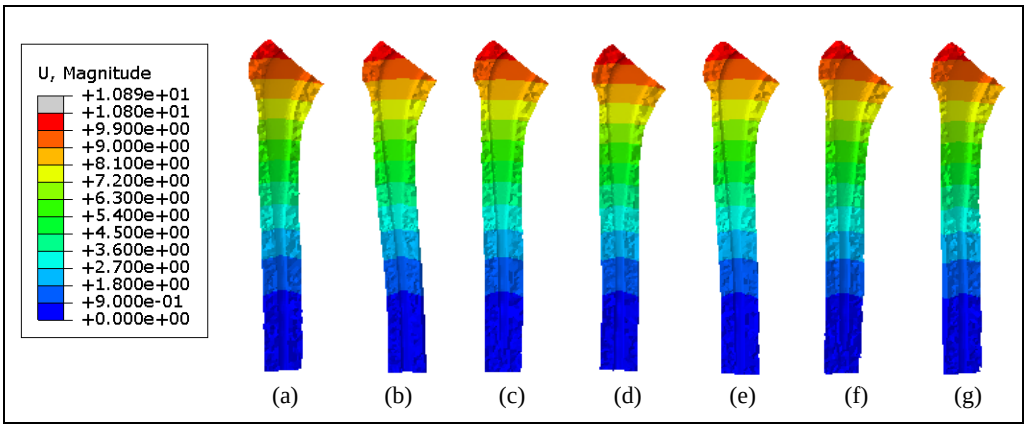

Fig. 8. Total deformation analysis for femoral bone at different varus angles (a) -0.75°, (b) -0.5°, (c) -0.25°, (d) 0°, (e) 0.25°, (f) 0.5°, and (g) 0.75°.

Besides, the colour display on the cement mantle remains consistent across all angles as shown in Fig 10 due to the von Mises stress values exhibiting minimal differences. The majority of the model exhibits a pronounced gradient of the blue colour, signifying lower values of von Mises stress. However, the pattern of stress distribution at -0.75° may show that stress is more evenly spread along the length of the cement mantle, and based on Fig 10, it exhibits minimum red colour compared to other angles. This could be interpreted as a more favourable condition for reducing the likelihood of localized cement failure. In Fig 11, where all the angles exhibit almost similar deformation patterns. This indicates that the cement mantle's response to the varus alignment within the tested range is relatively uniform. Furthermore, Fig 12, illustrates

https://doi.org/10.24191/jmeche.v22i1.2802

that the von Mises stress values fluctuate as the varus angle changes. Notably, there is a peak at -0.25° and -0.5°, suggesting these positions experience higher stress. There is a noticeable reduction in stress as the angle shifts from -0.25° to 0.25°, followed by a slight increase towards 0.75°. This pattern could suggest that certain angles are more prone to induce stress within the cement mantle, which could affect the longevity and stability of the implant. This may result from PMMA being softer facilitating the adaptation of implants and femurs to mitigate the strain transmitted from the implants to the femurs through deformation akin to a dashpot (Yavuz Solmaz et al., 2018). The magnitude of deformation gently decreases as the angle moves from -0.75° to 0.75° as shown in Fig 12. The changes are small but consistent. The smallest deformation is observed at 0.75°, indicating this may be a more stable configuration under the simulated conditions.

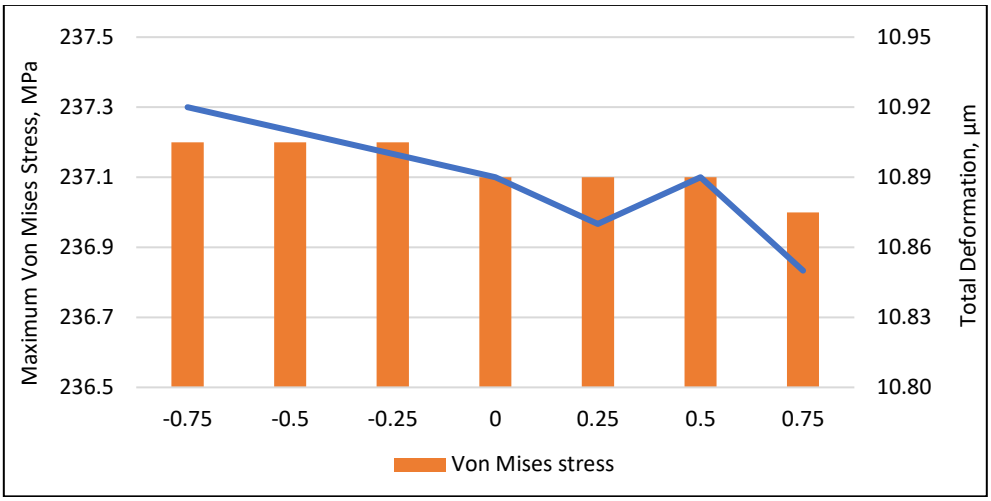

Fig. 9. Comparison of maximum von Mises stress and displacement for femoral bone at different varus angles.

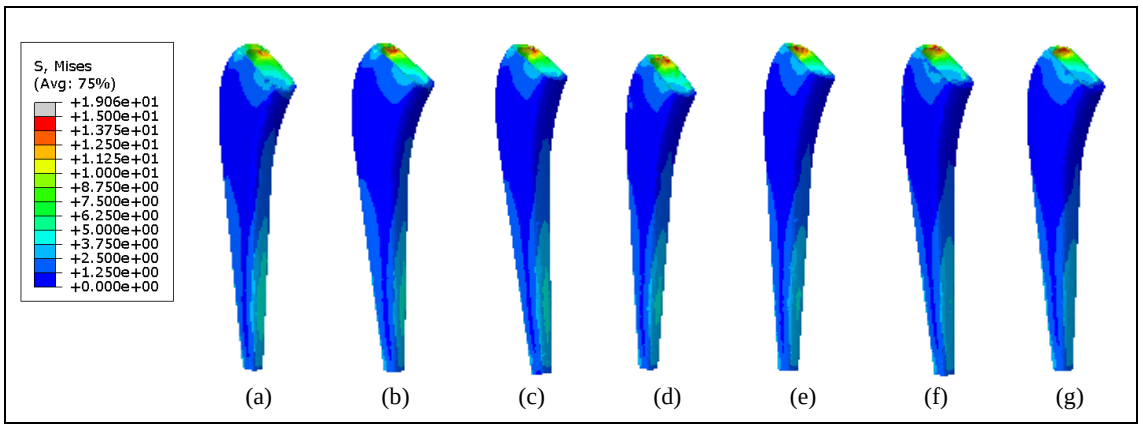

Fig. 10. Stress distribution analysis for cement mantle at different varus angles (a) -0.75°, (b) -0.5°, (c) -0.25°, (d) 0°, (e) 0.25°, (f) 0.5°, and (g) 0.75.

https://doi.org/10.24191/jmeche.v22i1.2802

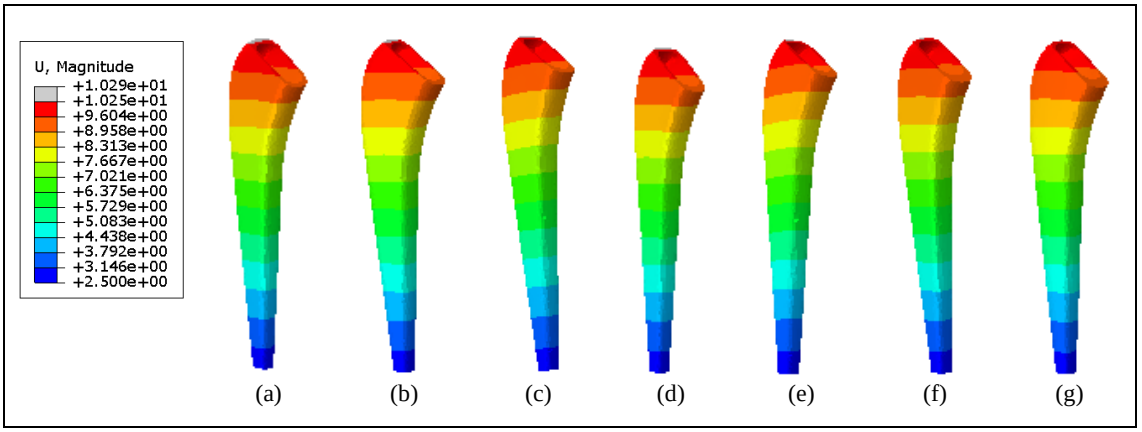

Fig. 11. Total deformation analysis for cement mantle different varus angles (a) -0.75°, (b) -0.5°, (c) -0.25°, (d) 0°, (e) 0.25°, (f) 0.5° and (g) 0.75°.

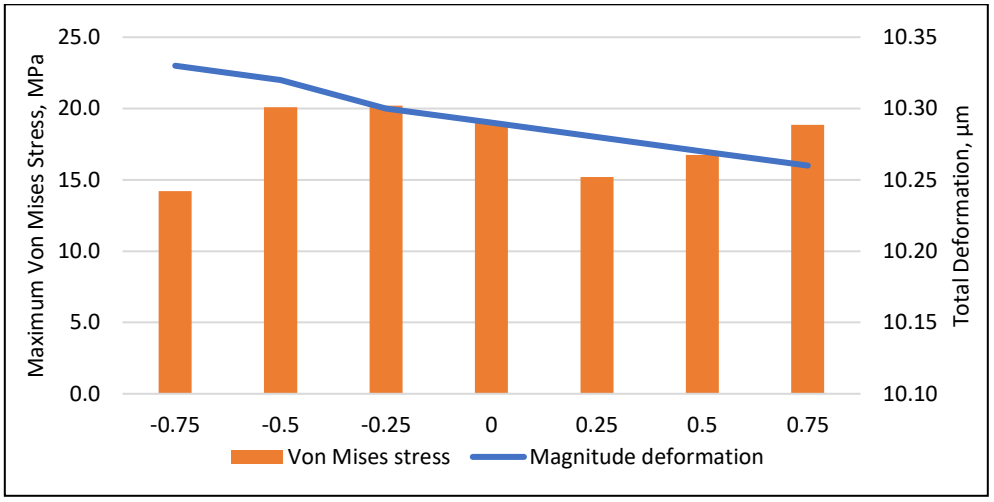

Fig. 12. Comparison of maximum von Mises stress and displacement for cement mantle at different varus angles.

Additionally, there is a slight colour gradient change across the angles which indicates a slight variation in stress distribution for the implant as shown in Fig 13. It can be seen that the red colour at the neck of an implant at 0.75° is more visible compared to others. While the overall pattern is almost similar, there may still be subtle differences in the extent of stress which could be important. These subtleties might not lead to immediate clinical issues but could have long-term implications for the integrity of the implant. Fig 14 shows the deformation experienced by the stem prosthesis at various angles of varus alignment. It displays a very subtle change in the color gradient across the angles, corresponding to the small changes in deformation. Specifically, the grayscale representation for the implant at 0.25°, 0.5°, and 0.75° angles is nearly imperceptible. This suggests that at these particular angles, the level of deformation experienced by the implant is notably lower, as denoted by the diminished visibility of grey tones in comparison to the surrounding color spectrum. Then, Fig 15 shows a slight but consistent increase as the angle moves from negative to positive. The stress increases from 188.3 MPa at -0.75° to 188.9 MPa at 0.75°. This trend suggests that the prosthesis experiences progressively higher stress as the angle deviates from the baseline

https://doi.org/10.24191/jmeche.v22i1.2802

position. The higher value of von Mises stress leads to the stress shielding phenomenon, which might result in aseptic loosening and instability of the implant (Yusof et al., 2021) .Besides, it also shows that the magnitude of deformation decreases slightly as the angle increases, from 11.33 μm at -0.75° to 11.27 μm at 0.75°. Even though the changes are minimal, there is a consistent trend where the deformation decreases as the angle becomes more positive.

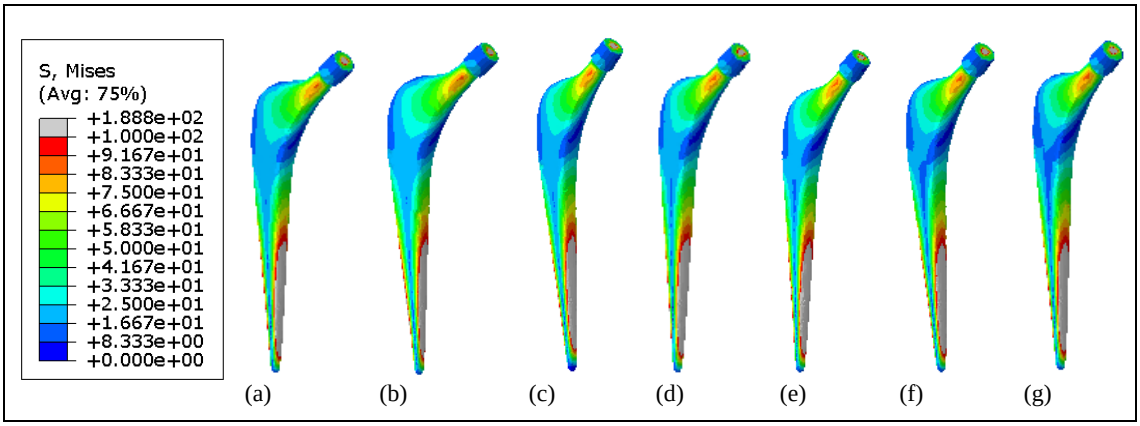

Fig. 13. Stress distribution analysis for implant at different varus angles (a) -0.75°, (b) -0.5°, (c) -0.25°, (d) 0°, (e) 0.25°, (f) 0.5° and (g) 0.75.

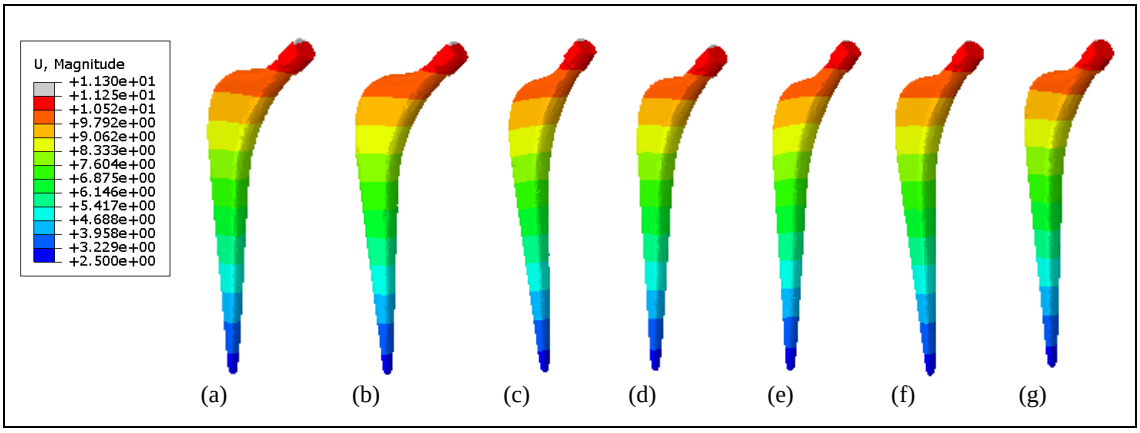

Fig. 14. Total deformation analysis for implant at different varus angles (a) -0.75°, (b) -0.5°, (c) -0.25°, (d) 0°, (e) 0.25°, (f) 0.5° and (g) 0.75°.

CONCLUSION

The development finite element model of cemented hip arthroplasty at varus implant positioning has been explored in this study. Furthermore, the effect of hip implant positioning has been analyzed through the distribution of stresses and total deformation. Several key findings can be drawn to conclude as follows:

https://doi.org/10.24191/jmeche.v22i1.2802

(i) The finite element analysis of varus alignment in cemented THA reveals that the baseline angle of 0° may not be the lowest stress and deformation in all components.

(ii) Varus angles show minimal influence on total deformation, with only a slight difference of 0.07 µm observed between the highest and lowest values for each component. However, they exhibit notable differences in von Mises stress values on the cement mantle, with the highest recorded at -0.25° (20.19 MPa) and the lowest at -0.75° (14.2 MPa).

(iii) Small changes in the varus angle do not significantly affect von Mises stress values within the femoral bone and implant. Optimal alignment may deviate from the traditional neutral position, as certain angles with deviations exhibit lower stress and deformation magnitudes.

Future studies should expand simulated physiological loads to include activities like walking and other daily motions, conducting multi-directional stress analyses to understand how cemented THA endures everyday activities. Considering material properties, particularly the condition of cement thickness due to hip stem alignment during the procedure, is crucial as it could influence stress distribution, ultimately aiming to reduce the risk of bone fracture and the quality of patients' life after THA.

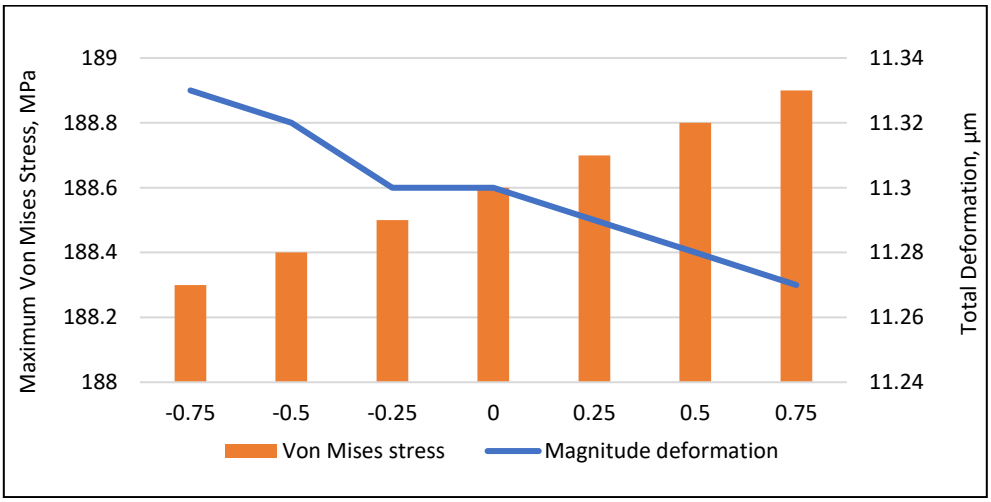

Fig. 15. Comparison of maximum von Mises stress and displacement for implant at different varus angles.

ACKNOWLEDGEMENT

The present study was conducted in collaboration with the University of Malaya, which provided crucial data for the study in developing the model and simulation.

CONFLICT OF INTEREST STATEMENT

All authors declare that they have no conflicts of interest.

https://doi.org/10.24191/jmeche.v22i1.2802

AUTHORS' CONTRIBUTIONS

The authors confirm their contribution to the paper as follows: **study design, simulation and initial draft**: Z.A. Aznan; **data collection, data analysis and initial draft**: N.M. Khairul Azahan; **software and reviewing**: S.H Marwan; **result interpretation and revision**: M. Taufiqurrakhman; **data interpretation and manuscript feedback**: H. Pandit; **writing-reviewing and editing**: T. Khan; **validation, supervision and editing**: A.H. Abdullah. All authors reviewed and approved the final version of this work.

REFERENCES

Abdelaal, M. S., Zachwieja, E., & Sharkey, P. F. (2021). Severe corrosion of modular dual mobility acetabular components identified during revision total hip arthroplasty. Arthroplasty Today, 8(3), 78–83. https://doi.org/10.1016/j.artd.2021.01.011

Ahmad, M. A., Zulkifli, N. N. M. E., Shuib, S., Sulaiman, S. H., & Abdullah, A. H. (2020). Finite element analysis of proximal cement fixation in total hip arthroplasty. International Journal of Technology, 11(5), 1046–1055. https://doi.org/10.14716/ijtech.v11i5.4318

Apostu, D., Lucaciu, O., Berce, C., Lucaciu, D., & Cosma, D. (2018). Current methods of preventing aseptic loosening and improving osseointegration of titanium implants in cementless total hip arthroplasty: A review. Journal of International Medical Research, 46(6), 2104-2119. https://doi.org/10.1177/0300060517732697

Bini, S. A., Chung, C. C., Wu, S. A., & Hansen, E. N. (2021). Tibial mechanical axis is nonorthogonal to the floor in varus knee alignment. Arthroplasty Today, 8, 237–242. https://doi.org/10.1016/j.artd.2021.03.009

Glenister, R., & Sharma, S. (2024). Anatomy, bony pelvis and lower limb, hip. StatPearls Publishing.

Gómez Alcaraz, J., Pardo García, J. M., Sevilla Fernández, J., Delgado Díaz, E., & Moreno Beamud, J. A. (2021). Primary total hip arthroplasty in elderly patients over 85 years old: Risks, complications and medium-long term results. Spanish Journal of Orthopedic Surgery and Traumatology, 65(1), 13–23. https://doi.org/10.1016/j.recot.2020.05.003

Jms, L., Ingle, P., Cheah, K., Dowell, J. K., & Mootanah, R. (2014). Total hip replacement: Tensile stress in bone cement is influenced by cement mantle thickness, acetabular size, bone quality, and body mass index. Journal of Computer Science & Systems Biology, 7(3), 72-78. https://doi.org/10.4172/jcsb.1000140

Katz, Y., Lubovsky, O., & Yosibash, Z. (2018). Patient-specific finite element analysis of femurs with cemented hip implants. Clinical Biomechanics, 58, 74–89. https://doi.org/10.1016/j.clinbiomech.2018.06.012

Kim, S.C., & Jung, H.M. (2013). A study on performance of low-dose medical radiation shielding fiber (RSF) in CT scans. International Journal of Technology, 4(2), 178–187.

Maggs, J., & Wilson, M. (2017). The relative merits of cemented and uncemented prostheses in total hip arthroplasty. Indian Journal of Orthopaedics, 51(4), 377–385. https://doi.org/10.4103/ortho.IJOrtho_405_16

Miller, R. E., Block, J. A., & Malfait, A. M. (2018). What is new in pain modification in osteoarthritis?. Rheumatology, 57(4), 99–107. https://doi.org/10.1093/rheumatology/kex522

https://doi.org/10.24191/jmeche.v22i1.2802

Mitsutake, R., Tanino, H., Nishida, Y., Higa, M., & Ito, H. (2020). A simple angle-measuring instrument for measuring cemented stem anteversion during total hip arthroplasty. BMC Musculoskeletal Disorders, 21(1), 113. https://doi.org/10.1186/s12891-020-3142-7

Ng, K. C. G., Jeffers, J. R. T., & Beaulé, P. E. (2019). Hip joint capsular anatomy, mechanics, and surgical management. The Journal of Bone and Joint Surgery, 101(23), 2141–2151. https://doi.org/10.2106/JBJS.19.00346

Olugbade, T. O. (2022). Stainless steels. In A. Singh (Ed.), Corrosion Resistance, Evaluation Methods, and Surface Treatments of Stainless Steels (pp. 1-7). IntechOpen.

Ramanathan, S., Lin, Y. C., Thirumurugan, S., Hu, C. C., Duann, Y. F., & Chung, R. J. (2024). Poly(methyl methacrylate) in orthopedics: Strategies, challenges, and prospects in bone tissue engineering. Polymers, 16(3), 367. https://doi.org/10.3390/polym16030367

Rivière, C., Lazic, S., Dagneaux, L., Van Der Straeten, C., Cobb, J., & Muirhead-Allwood, S. (2018). Spine-hip relations in patients with hip osteoarthritis. EFORT Open Reviews, 3(2), 39–44. https://doi.org/10.1302/2058-5241.3.170020

Schwab, J. H. (2017). Global sagittal alignment. Skeletal Radiology, 46(12), 1613–1614. https://doi.org/10.1007/s00256-017-2752-0

Tamaki, Y., Goto, T., Iwase, J., Wada, K., Hamada, D., Tsuruo, Y., & Sairyo, K. (2022). Contributions of the ischiofemoral ligament, iliofemoral ligament, and conjoined tendon to hip stability after total hip arthroplasty: A cadaveric study. Journal of Orthopaedic Research, 40(12), 2885–2893. https://doi.org/10.1002/jor.25320

Torini, A. P., Barsotti, C. E., Andrade, R. M., Nali, L. H. d. S., & Ribeiro, A. P. (2023). Effect of total hip arthroplasty with ceramic acetabular component on clinical, radiographic and functional parameters in older patients with hip osteoarthritis: Two-year follow-up. Journal of Clinical Medicine, 12(2), 670. https://doi.org/10.3390/jcm12020670

Whittaker, J. L., Runhaar, J., Bierma-Zeinstra, S., & Roos, E. M. (2021). A lifespan approach to osteoarthritis prevention. Osteoarthritis and Cartilage, 29(12), 1638–1653. https://doi.org/10.1016/j.joca.2021.06.015

Yavuz Solmaz, M., Hakki Sanliturk, I., Turgut, A., Dundar, S., & Topkaya, T. (2018). Stress distribution in a femoral implant with and without bone cement and at different inclination angles. Materials Testing, 60(4), 393–398.

Yue, L., & Berman, J. (2022). What is osteoarthritis?. Journal of the American Medical Association, 327(13), 1300. https://doi.org/10.1001/jama.2022.1980

Yusof, M. S., Aznan, N., Abdul Manan, N. F., Marwan, S. H., Mazlan, M. H., & Abdullah, A. H. (2021). Effects of varus and sagittal implant positioning to the stress adaptation in cementless hip arthroplasty. Malaysian Journal of Medicine and Health Sciences, 17(13), 22-27.

Zheng, Z., Chen, S., Liu, X., Wang, Y., Bian, Y., Feng, B., Zhao, R., Qiu, Z., Sun, Y., Zhang, H., Cui, F., Yang, X., & Weng, X. (2021). A bioactive polymethylmethacrylate bone cement for prosthesis fixation in osteoporotic hip replacement surgery. Materials and Design, 209, 109966. https://doi.org/10.1016/j.matdes.2021.109966

https://doi.org/10.24191/jmeche.v22i1.2802